Topological Repair on Voxel-Based Quadrangular Meshes

Paulette Lieby[1], Nick Barnes[1], and Brendan D. McKay[2]

[1] Vision Science, Technology and Applications, Canberra, National ICT Australia,
Paulette.Lieby@anu.edu.au, Nick.Barnes@nicta.com.au
[2] Department of Computer Science, Australian National University,
bdm@cs.anu.edu.au

Abstract. In some neuroscience applications it is critical that the representation of anatomical structures is topologically faithful. This is especially important when the topology is known to be equivalent to a sphere. We propose a new approach to repair a voxel-based quadrangular mesh so that it becomes topologically equivalent to a sphere. The approach is graph-based and results in practice in an amount of change that is generally minimal. The algorithm was successfully applied to a database of 977 hand-segmented hippocampi from a study of ageing; spherical topology was achieved for all data sets.

1 Introduction

In medicine and neuroscience, the faithful recovery of anatomical structures from 3D voxel-based image data is an important goal. Some of these structures are known to be topologically equivalent to a sphere, that is, they can be mapped onto a sphere by continuous deformation. This is the case for the cortical surface [1, 2], the hippocampus [3, 4], and the lateral ventricle [5].

A spherical topology guarantees the existence of an invertible one-to-one map between such structures. This facilitates analysis between subjects using surface warping [6] and it simplifies registration. However, artifacts may be introduced in the recovery of these structures by hand-tracing or automatic recovery processes. In the case of both hippocampus and cortical surface, for normal neuroanatomy, artifacts such as handles and isolated voxels do not reflect the true neuroanatomical structure. This may cause problems for some applications such as warping, registration, and some forms of mathematical modelling (e.g., spherical harmonic mapping [3, 7, 4, 5]). In this case, it is important for the voxel-based data to reflect the spherical topology.

In this paper we present an algorithm for topological repair, focusing on the detection of handles and how to repair them. The traditional approach to topological repair is human intervention (e.g. [8]). Common recent approaches involve isosurface reconstruction with topological control using fast marching methods ([9, 10]), watersheds ([11]), morphological operators ([12]). Others focus on repairing the surface tessellation itself ([13]). Yet other approaches are graph-based and they also operate directly on the digital volume ([1, 2]). The aim of

all these methods (except [13]) is to repair the volume so that after applying a topologically consistent isosurface algorithm, Marching Cubes tessellation for example, one obtains a triangulation with spherical topology.

However, triangulation is less suitable if further analysis is required, such as shape analysis, or if the aim is to generate a model where we require precise correspondence with the original grey-level data (e.g. [3]). Correspondences are trivially preserved by a voxel-based mesh, but this is not obvious in the case of Marching Cubes tessellation. Further, a voxel-based mesh may be uniformly mapped on the sphere, thus enabling the computation of the shape's spherical harmonics ([7]). Finally, hand-tracings are generally performed as precisely as possible, so it is preferable to stay close to the hand-segmented data as a general principle.

Other approaches have also corrected the topology within a voxel-based representation, for example [14]. However in this case it is not clear if defects can be detected automatically. A method described by [15] applies smoothing and level-set filters on the surface. However, such operations are not guaranteed to find all handles, and may change a large number of voxels.

Our approach is graph-based, operates on the digital volume and produces a voxel-based quadrangulation as the resulting surface mesh. We apply a fundamental result from algebraic topology to detect handles directly in the surface mesh. We are then able to correct all well-behaved small handles, usually in a minimal way.

The paper is divided as follows. The next section outlines the major steps of our approach while Sections 3 to 6 explore each step in detail. In Section 7 we discuss the algorithm's performance as applied to a database of 977 hand-traced hippocampi and in Section 8 we examine the strengths and shortcomings of our approach.

2 Approach

Three-dimensional segmented digital data is a binary image that distinguishes the *interior* (foreground) voxels from the *exterior* (background) voxels. The *surface mesh* consists of the voxel corners, edges, and faces lying on the boundary between interior and exterior. A voxel corner, edge, or face on the surface mesh is called a *vertex*, an *edge* or a *face* respectively.

A vertex v is *adjacent* to vertex u if there is an edge between u and v. We say that v is a *neighbour* of u and conversely. The surface mesh is a description of the surface which, for each vertex v, lists the neighbours of v in an orderly way (see Section 4). Since every face is bordered by four edges, the surface mesh is said to be a *quadrangulation*.

Our method to produce a topologically correct surface from the hand-segmented data can be described as follows:

1. At each vertex on the surface, apply a correction filter on the original binary volume data to ensure that the surface at this vertex is non-self-intersecting (Figure 1(a)).

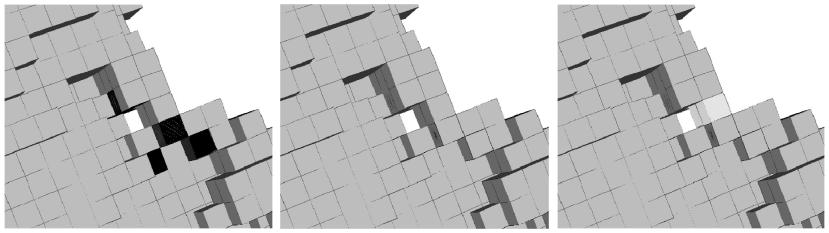

(a) (b) (c)

Fig. 1. A partial view of a surface mesh for a hand-segmented hippocampus. (*a*) After application of the correction filter, the dark voxels have been added; (*b*) The surface mesh; (*c*) Topological repair: the light voxels are marked for removal to open the handle.

2. From the non-self-intersecting surface, construct the surface mesh (Figure 1(*b*)).
3. Use the surface mesh to locate any handles.
4. Convert the handle into sets of voxels to be either removed or added.
5. Repair the topology by either filling the tunnel or opening the handle (Figure 1(*c*)).

Each of these points is addressed in the subsequent sections.

3 The Correction Filter

In order for a surface to be topologically equivalent to a sphere it must be non-self-intersecting. This is equivalent to saying that it is locally homeomorphic to a disk. Figure 2 shows the three fundamental obstructions for the surface to being locally homeomorphic to a disk. See [16] for a proof.

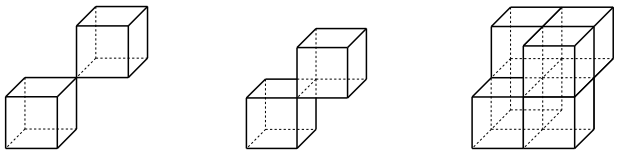

Fig. 2. The forbidden configurations

At each vertex, we determine if any configuration in Figure 2 is present; this is achieved by a simple case by case examination. The forbidden configuration is removed by either adding and removing the minimum number of voxels that renders the surface non-self-intersecting at this vertex.

This correction filter is applied to each vertex in order, where the vertices are ordered lexicographically on their coordinates. While applying the filter at some

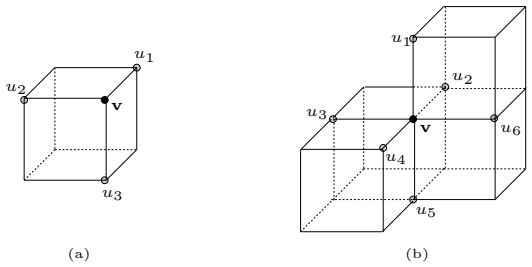

Fig. 3. Neighbours of v in anti-clockwise order. (a): u_1, u_2, u_3; (b): $u_1, u_2, u_3, u_4, u_5, u_6$

vertex v, one has to be careful not to introduce new forbidden configurations which did not originally exist. This is achieved by recursively examining all vertices whose neighbourhood has been affected and who are less than or equal to v (in the sense of the order described above). It is easy to see that this process must terminate.

It is possible that the application of the filter results in the formation of topological defects; they will be corrected as explained in Sections 5 and 6.

Note also that the application of the correction filter to all vertices of the hand-segmented data results in a *6-connected* 3D digital image. A digital image is said to be 6-connected when two voxels are neighbours if and only if they share a common face.

4 Mesh Creation

Once the surface is non-self-intersecting we construct the surface mesh consisting of the surface vertices and edges. As mentioned in Section 2 the list of neighbours of a given vertex is given in an *orderly* way.

Choose a direction, say, anti-clockwise. Given a vertex v, the ordered list of neighbours of v is $u_1, u_2, \ldots, u_n$ where the sequence of vertices is given by the direction of traversal of the neighbours of v. See Figure 3 for an example. Note that the starting vertex of the list is irrelevant.

To construct the surface mesh, for each vertex v on the surface, we perform an anti-clockwise walk starting at v and visiting all the neighbours of v. Two steps are necessary to ensure that we traverse the list of neighbours of v in a consistent fashion (e.g. always anti-clockwise). First we assign a normal to each face in a consistent manner (e.g. pointing towards the *exterior* of the object). Secondly, we ensure that the cross-products of the vectors that describe the walk have the same direction relative to the assigned face normal.

Let u_1 and u_2 be neighbours of v such that the path of vertices v, u_1, v_0, u_2 describes a anti-clockwise walk around the face f incident to v, u_1 and u_2 (see Figure 4 (a) for an example). The vertex v_0 is the vertex of this face which is not adjacent to v, i.e. there is no edge between v and v_0. Then the cross-products

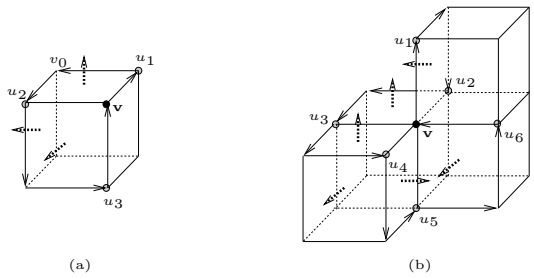

Fig. 4. Anti-clockwise walk around vertex v starting at u_1. Normals are indicated by the thick dashed arrows.

$\overrightarrow{(u_1 - v)} \times \overrightarrow{(v_0 - u_1)}$, $\overrightarrow{(v_0 - u_1)} \times \overrightarrow{(u_2 - v_0)}$, and $\overrightarrow{(u_2 - v_0)} \times \overrightarrow{(v - u_2)}$ all have the same direction as the normal of the face f. This is depicted in Figure 4.

5 Locating Handles

At this point, the surface of the object is fully described by its surface mesh, enumerating the vertices and the sequence of their neighbours. We may always assume that the mesh is connected. The aim is to obtain a mesh which is topologically equivalent to a sphere.

Given a connected surface mesh with n vertices, m edges and l faces, the *genus* g of the surface is given by Euler's formula ([17])

$$g = \frac{1}{2}(2 - n + m - l).$$

The genus measures the number of *handles* of the surface. For example, a sphere has no handles, while a torus has one handle. We name the hole surrounded by a handle a *tunnel*, see Figure 5(c).

A fundamental result of algebraic topology ([17]) states that there is a handle in the surface mesh *if and only if*

1. there are two cycles A and B in the mesh such that A and B intersect at v;
2. and, walking along B to cross A at v results in moving from the "left" to the "right" of A without encountering any other vertex of A ("left" and "right" of A are relative to an arbitrary direction assigned to A).

This is shown in Figure 5.

Let us call cycles that have the property pictured in Figure 5 (b) and (c) *interlocking cycles* or *interlocking cycles at* v. We also say that B is the *transverse* of A and conversely.

We locate the handles by finding interlocking cycles in the surface mesh. In order to achieve a minimum amount of change we must find the smallest interlocking cycles. This is easily done by performing a breath-first-search on

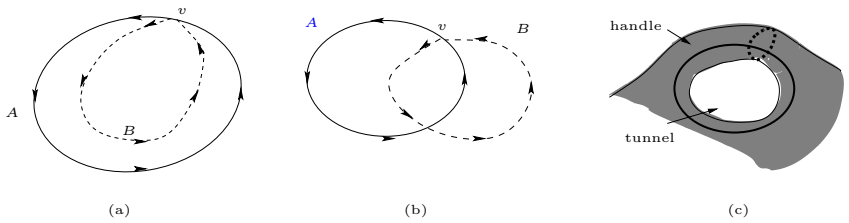

Fig. 5. In (*a*) A and B are intersecting and B is entirely on one "side" of A; this is not a handle. In (*b*) and (*c*) A and B are intersecting but B starts and ends at opposite sides of A; this is a handle.

the mesh. The fact that the neighbours of each vertex are given in an orderly fashion (Section 4) enables us to determine if cycles are interlocking.

6 Converting Handles to Sets of Voxels

Once interlocking cycles are found they are converted into sets of voxels that describe the handle to be opened or the tunnel to be filled in order to correct the topological defect. Henceforth we only discuss handles since tunnels are dealt with in a similar way, but with background voxels replacing foreground voxels. The equivalence between handles and tunnels arises from the fact that the surface is non-self-intersecting.

Let $[A, B]$ be a pair of interlocking cycles at v. Let C be one of A or B and assume that C is a cycle of vertices $v_1, v_2, \ldots, v_n$ where v_1 and v_n are actually the same vertex v. Along C construct a set P of voxels $u_1, u_2, \ldots, u_m$ such that: $u_1 = u_m$; u_j has a common face with some u_k with $1 \leq k < j$, $1 < j \leq m$; each edge (v_i, v_{i+1}) in C, $1 \leq i < n$, is adjacent to a voxel u_j in P; and, each voxel u_j in P is adjacent to an edge in C.

Now, in order for the set P to properly open a handle, it must also have genus zero. If C is small then P is likely to have genus zero (see Figure 6), but it is not difficult to see that when C is large, then P itself may possess handles. One remedy to this situation is to fill the handles of P by examining each pair of consecutive voxels u_j and u_{j+1} in P and deduce from it which voxel should be added. Once P is obtained from C and P has genus zero then one decides if removing the voxels in P (in case of a handle) or adding them (in case of a tunnel) properly corrects the topology (see Figure 6). This is easily verified by counting the vertices, edges and faces of the corresponding digital image and applying Euler's formula. After repair we need to run the correction filter on the vertices incident to these voxels to ensure that the newly obtained surface is non-self-intersecting.

Figure 7 shows the result of applying the algorithm to a segmented hippocampus. Dark voxels are those added and light voxels are those removed as a

result of applying the correction filter and the topological repair routine. Notice how the handle has been broken up.

Finding the initial set P along C is easy but may be expensive as there may be many different solutions. We always choose the smallest. Filling the handles of P, if P is not already topologically equivalent to a sphere, is harder and may not succeed in rendering P topologically correct. Similarly, we may not succeed in finding a set P such that P corrects the topology. In this case we reject P and try another path of voxels P along cycle C. If no appropriate set P can be found for either cycle A or B in the $[A, B]$ pair, we examine another pair of interlocking cycles at v. All the cycles belonging to pairs of interlocking cycles at v are considered in non-increasing order of size, thus ensuring that, at a given vertex v, we find the minimal set P that repairs the topological defect. If there is a handle in the neighbourhood of a given vertex v, there are many cycles passing through v, and given a cycle C through v, there are many transverses of C through v. Figure 6 shows how different transverses are found for the same cycle.

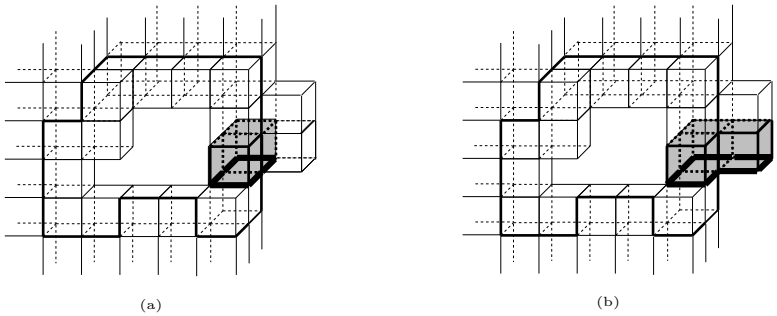

Fig. 6. The cycle in (a) does not succeed in finding an appropriate set of voxels to break the handle, while the one in (b) does.

7 Experiment

We have used the algorithm to successfully compute a topologically correct voxel-based surface mesh on all valid 977 hand-segmented hippocampi in the database resulting from a longitudinal study on ageing, The PATH Through Life Project, conducted by the Centre for Mental Health Research at the Australian National University, Canberra. One hippocampus among the data set of 977 is shown in Figure 7.

As can be seen from Section 3 and especially from Section 6 the proposed algorithm is potentially exponential in time with respect to the number of vertices on the surface. However for all practical purposes the algorithm corrects the surface in a reasonable time. Over the whole data set and on a 3.2GHz Pentium 4 processor, it spends on average 40.77 seconds processing 2977 voxels.

Of the 977 hand-segmented hippocampi, 271 present a non-zero genus surface with 378 handles in total. It takes on average 82.24 seconds to correct each data set processing an average volume of 2932 voxels, and it takes 2.57 voxels to correct each handle. When considering the total number of modified voxels (that is, including those modified as a result of the correction filter) on average 23.47 voxels are changed over all the 977 data sets.

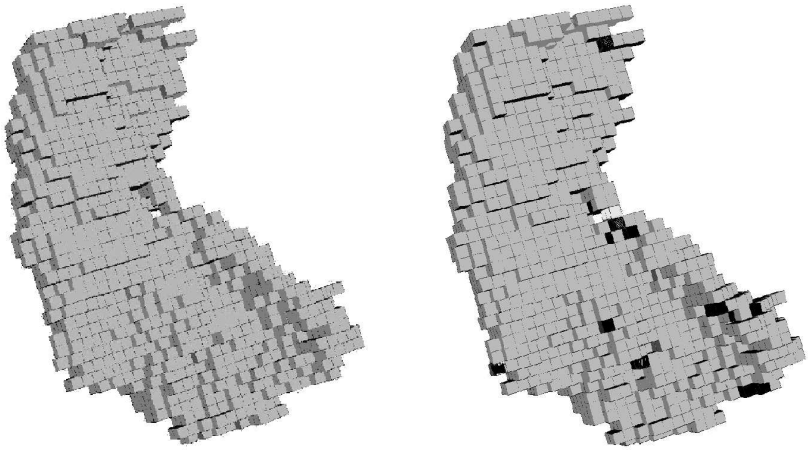

Fig. 7. Left: A segmented hippocampus: original digital data. Right: The hippocampus with spherical topology realised; Dark voxels are those added and light voxels are those removed. Notice how the handle has been broken up.

8 Discussion

One issue raised in Section 6 is the possibility of the algorithm not being able to find a set of voxels that correctly repairs the topology. Our experiment shows that we can successfully deal with anatomical data with small defects. This is consistent with our approach where difficulties may arise only when the size of the topological defect becomes significantly large. Figure 8 lists the size of the corrections effected together with their frequencies.

Size of handle corrections	1	2	3	4	5	6	7	8	9	10	11	
Frequencies	100	131	69	37	19	12	3	1	3	2	1	378

Fig. 8. Size of handle corrections and their frequencies.

There is also the difficulty of effecting topological repair by modifying a minimum number of voxels. As can be seen from the order in which we examine interlocking cycles we may not necessarily guarantee a minimal amount of change since a handle may be described by cycles interlocking at more than one vertex. Our strategy is principally guided by considerations of time and space efficiency and by the assumption that topological defects remain small.

The strengths of the proposed algorithm are its simplicity and the fact that it makes no assumption about the digital data, except that the object input is connected. In particular, as opposed to [2], one does not require that the input data be 6-connected.

The simplicity of the algorithm lies in the way handles are located. Finding interlocking cycles at a given vertex v is linear in the size of the handle present in the vicinity of v. When no handle is present the search is quadratic in s, the size of the largest handle in the surface. In practice, one terminates the search after a preset value s has been reached.

Finally, an important feature of the proposed algorithm is that it produces a voxel-based quadrangulation, as opposed to a Marching Cubes tessellation [9–11, 13, 1, 2]. This is necessary when intending to compute the shape's spherical harmonics, as the quadrangulation's vertices can be uniformly mapped onto the sphere, ensuring a faithful reconstruction using from harmonic series.

Our algorithm could be improved in at least two ways. Firstly we need to find a more robust means of converting a cycle of edges in the surface into a minimal set of voxels that repairs the topology. In this regard it might be helpful to investigate some of the ideas in [14]. These ideas may also help in reducing the algorithm's complexity, which principally arises from the attempt at repairing the discovered defects. Secondly and lastly, we may think of a different strategy for choosing interlocking cycles to ensure minimum change.

In the future we wish to test our algorithm on cortical surfaces; they are known to be topologically equivalent to a sphere and their reconstructed surface usually shows many topological defects ([1, 2, 18]). The defects are typically small so one would expect our algorithm to perform well. Of interest will be to investigate how the changes in volume resulting from the application of the correction filter and the repair routine compare with techniques described in [1, 2].

Acknowledgments

National ICT Australia is funded by the Australian Department of Communications, Information Technology and the Arts and the Australian Research Council through *Backing Australia's ability* and the ICT Centre of Excellence Program.

The authors thank K. Anstey, C. Meslin, J. Maller, and the PATH research team at the Centre for Mental Health Research, Australian National University, Canberra, and P. Sachdev, Neuropsychiatric Institute, University of New South Wales, Sydney, for providing the original MR and segmented data sets.

The authors would also like to thank M. Styner for a helpful exchange.

References

1. Han, X., Xu, C., Braga-Neto, U., Prince, J.: Topology Correction in Brain Cortex Segmentation Using a Multiscale, Graph-Based Algorithm. IEEE Transactions on Medical Imaging **21**(2) (2002) 109–121
2. Shattuck, D., Leahy, R.: Automated Graph-Based Analysis and Correction of Cortical Volume Topology. IEEE Transactions on Medical Imaging **20**(11) (2001) 1167–1177
3. Keleman, A., Szekely, G., Gerig, G.: Elastic Model-Based Segmentation of 3D Neuroradiological Data Sets. IEEE Trans. Medical Imaging **18**(10) (1999) 828–839
4. Styner, M., Lieberman, J., Pantazis, D., Gerig, G.: Boundary and Medial Shape Analysis of the Hippocampus in Schizophrenia. Medical Image Analysis **8** (2004) 197–203
5. Styner, M., Lieberman, J., McClure, R., Weingberger, D., Jones, D., Gerig, G.: Morphometric Analysis of Lateral Ventricles in Schizophrenia and Healthy Controls Regarding Genetic and Disease-Specific Factors. In: Proceedings of the National Academy of Science. Volume 102. (2005) 4872–4877
6. Thompson, P., Moussai, J., Zohoori, S., Goldkorn, A., Khan, A., Mega, M., Small, G., Cummings, J., Toga, A.: Cortical Variability and Asymmetry in Normal Aging and Alzheimer's disease. Cereb. Cortex **8**(6) (1998) 492–509
7. Brechbühler, C., Gerig, G., Kübler, O.: Parametrization of Closed Surfaces for 3-D Shape Description. Computer Vision and Image Understanding **61**(2) (1995) 154–170
8. Fischl, B., Sereno, M., Dale, A.: Cortical Surface-Based Analysis II: Inflation, Flattening, and a Surface-Based Coordinate System. NeuroImage **9** (1999) 195–207
9. Bazin, P., Pham, D.: Topology correction using Fast Marching Methods and its Application to Brain Segmentation. In: MICCAI. (2005)
10. Jaume, S., Rondao, P., Macq, B.: Open Topology: A Toolkit for Brain Isosurface Correction. In: MICCAI. (2005)
11. Couprie, M., Najman, L., Bertrand, G.: Quasi-Linear Algorithms for the Topological Watershed. Journal of Mathematical Imaging and Vision **22**(2-3) (2005) 231–249
12. Bischoff, S., Kobbelt, L.: Isosurface Reconstruction with Topology Control. In: 10th Pacific Conference on Computer Graphics and Applications. (2002) 246
13. Segonne, F., Grimson, E., Fischl, B.: A Genetic Algorithm for the Topology Correction of Cortical Surfaces. In: In Proceedings of Information Processing in Medical Imaging, LNCS. Volume 3565. (2005) 393–405
14. Aktouf, Z., Bertrand, G., Perroton, L.: A Three-Dimensional Holes Closing Algorithm. Pattern Recognition Letters **23**(5) (2002) 523–531
15. (Styner, M.) Personal communication.
16. Abrams, L., Fishkind, D., Priebe, C.: The Generalized Spherical Homeomorphism for Digital Images. IEEE Transactions on Medical Imaging **23**(5) (2004) 655–657
17. Lawson, T.: Topology: A Geometric Approach. Oxford University Press (2003)
18. Fischl, B., Sereno, M., Dale, A.: Cortical Surface-Based Analysis I: Segmentation and Surface Reconstruction. NeuroImage **9** (1999) 179–194